

## Coordinated reel adjustment based on 3D rapeseed plant structure for loss reduction<sup>1</sup>

### Ajuste coordenado do molinete com base na estrutura da planta de canola 3D para redução de perdas

Yanbin Liu<sup>2\*</sup>, Yaoming Li<sup>2</sup>, Tiaotiao Chen<sup>2</sup>, Zhenwei Liang<sup>2</sup> & Li Zeng<sup>3</sup>

<sup>1</sup> Research developed at Inner Jiangsu University, College of Agricultural Engineering, Zhenjiang, Jiangsu, China

<sup>2</sup> Jiangsu University/College of Agricultural Engineering, Zhenjiang, Jiangsu, China

<sup>3</sup> Shandong Golddafeng Machinery Company Limited, Jining, Shandong, China

#### HIGHLIGHTS:

*Variation in quantity of rapeseed plant height and center of gravity height is different.*

*The 3D structural characteristic of the same variety of rapeseed plant (e.g., plant height) is changeable.*

*Striking the pods on upper layer of main stalk and top part branches should be reduced.*

**ABSTRACT:** The reel motion trajectory of the traditional rapeseed combine harvester is unable to adapt to the characteristics of rapeseed plants, leading to high reel rapeseed loss. In this study, the “Ningza 158” rapeseed variety—during the optimum harvest period—was selected as the research object, with a sample size of 25. From early May to mid-July 2024, the correlation between the three-dimensional (3D) structural characteristic parameters of rapeseed plants and the difference in the pod characteristic parameters at different growing positions of a single rapeseed plant was analyzed using statistical methods, which provided an important theoretical basis for improving the adaptability of the reel to the characteristics of rapeseed plants. The results showed that, above the stubble height, the center of gravity height of rapeseed plants was approximately 8/13 of the plant height, and the variation coefficient of the relative position was 4.0%. The variation coefficient of the 3D structural characteristic parameters ranged from 9.3 to 41.9%, indicating that the characteristic was complex and highly variable. Based on a criterion of a correlation coefficient  $\geq 0.8$ , nine linear regression models among different 3D structural characteristic parameters were established. It was necessary to improve the adaptability of the reel to the change in plant height by coordinating the adjustment of the installation height and the diameter of the reel. Striking the pods on the upper layer of the main stalk and top part branches should be reduced in the reel operation, which would be helpful in diminishing reel rapeseed loss.

**Key words:** *Brassica napus* L., plant morphology, combine harvester, header loss, reel optimization

**RESUMO:** A trajetória de movimento do molinete da colheitadeira tradicional de canola não consegue se adaptar às características da planta de canola, resultando em alta perda de grãos durante a operação. Neste estudo, a variedade de canola “Ningza 158” no período ideal de colheita foi selecionada como objeto de pesquisa, com um tamanho de amostra de 25 plantas. Entre o início de maio e meados de julho de 2024, a correlação entre os parâmetros característicos da estrutura tridimensional (3D) da planta de canola e a diferença nos parâmetros característicos das vagens em diferentes posições de crescimento de uma única planta foi analisada por métodos estatísticos, o que forneceu uma base teórica importante para melhorar a adaptabilidade do molinete às características da canola. Os resultados mostraram que, acima da altura do restolho, a altura do centro de gravidade da canola foi de aproximadamente 8/13 da altura da planta, e o coeficiente de variação da posição relativa foi de 4,0%. Os coeficientes de variação dos parâmetros característicos da estrutura 3D variaram de 9,3 a 41,9%, indicando que as características são complexas e altamente variáveis. Com base no critério de coeficiente de correlação  $\geq 0,8$ , foram estabelecidos nove modelos de regressão linear entre diferentes parâmetros característicos da estrutura 3D. Foi necessário melhorar a adaptabilidade do molinete à variação da altura das plantas por meio do ajuste coordenado da altura de instalação e do diâmetro do molinete. Deve-se reduzir o impacto nas vagens localizadas na camada superior do caule principal e dos ramos superiores durante a operação do molinete, o que ajudará a reduzir as perdas de grãos.

**Palavras-chave:** *Brassica napus* L., morfologia vegetal, colheitadeira, perda na plataforma de corte, otimização do molinete

## INTRODUCTION

Rape (*Brassica napus L.*) is one of the most important oil crops in the world (Delgado et al., 2021; Shu et al., 2022; Guo et al., 2024; Wang et al., 2024), and the main mechanized method employed for harvesting it is through the use of a combine harvester (Tang et al., 2021a, 2021b; Hu et al., 2024; Que et al., 2024). However, there is a high level of rapeseed loss when utilizing this method (Qing et al., 2021a; Luo et al., 2025; Sun et al., 2025).

The loss of rapeseed as a result of using a combine harvester mainly involves header, and threshing and cleaning, losses, with the former accounting for more than 50% of the total (Qing et al., 2021b). This is because the reel, which is located at the very front of the combine harvester and is equipped with sprung teeth, strikes the rapeseed plant, which can easily cause pods to shatter (Ma et al., 2020; Li et al., 2024).

Research on the characteristics of crop plants provides a key theoretical basis for improving the performance of combine harvesters (Ji et al., 2022; Zhao et al., 2022; Du et al., 2023; Jing et al., 2024; Zhou et al., 2026); however, while studies on rapeseed plant characteristics have supported harvester design (Qing et al., 2021b; Yuan et al., 2022), the 3D structure of the plant and its pod characteristics at different growing positions remain poorly studied.

It has been hypothesized that significant correlations exist between the 3D structural parameters of the rapeseed plant and the fact that pod characteristics vary significantly across different growing positions. Furthermore, it has also been suggested that these variations and correlations are key factors that are not currently taken into account in reel design, leading to poor adaptability of the reel motion trajectory to the complex plant structure.

Therefore, in this study, the relevant parameters affecting the 3D structural characteristic of rapeseed plants and pod characteristics were measured, and statistical methods were used to analyze the measurement data. The objective of this study was to provide a theoretical basis for improving the adaptability of reels to complex and variable rapeseed plant structures, with a view to reducing header loss.

## MATERIAL AND METHODS

This study was conducted from early May to mid-July 2024 at two key sites in Zhenjiang City, Jiangsu Province, China (~32°N, 119°E, elevation 6–10 m), namely the Shiyezhou experimental field (Figure 1), which was irrigated using furrow irrigation, and Jiangsu University. The “Ningza 158” brassica rape variety was selected as the research object due to its status as the predominant cultivar in the local region. The planting method adopted was mechanical direct seeding, with a row spacing of 0.4 m, and the average planting density was 30–35 plants per m<sup>2</sup>. The period between the yellow ripening stage and the full ripening stage in rapeseed plants, when more than 90% of the rape pods in the field turn yellow and brown, is considered the optimum time for harvesting rape with a combine harvester. Plant sampling was performed on May 7, 2024, when the weather was overcast

to clear and temperatures ranged from 15 to 27 °C. The five-point sampling method prescribes that the area of each sampling point should be 1 m<sup>2</sup>, with five undamaged rapeseed plants being randomly selected from each point. The stubble height of the rape combine harvester is generally about 0.35 m (Qing, 2021), so the cut sample is taken and marked at 0.35 m above the ground.

The shape and density of rapeseed plants during the harvest period are irregular and uneven; therefore, above the stubble height, the relative position of the center of gravity height (C) is measured for ten rapeseed plants using the suspension method. The center of gravity is defined by this method as the intersection point of two plumb lines dropped from different suspension points. The equation for calculating C is as follows:

$$C = \frac{G_h}{H} \quad (1)$$

where:

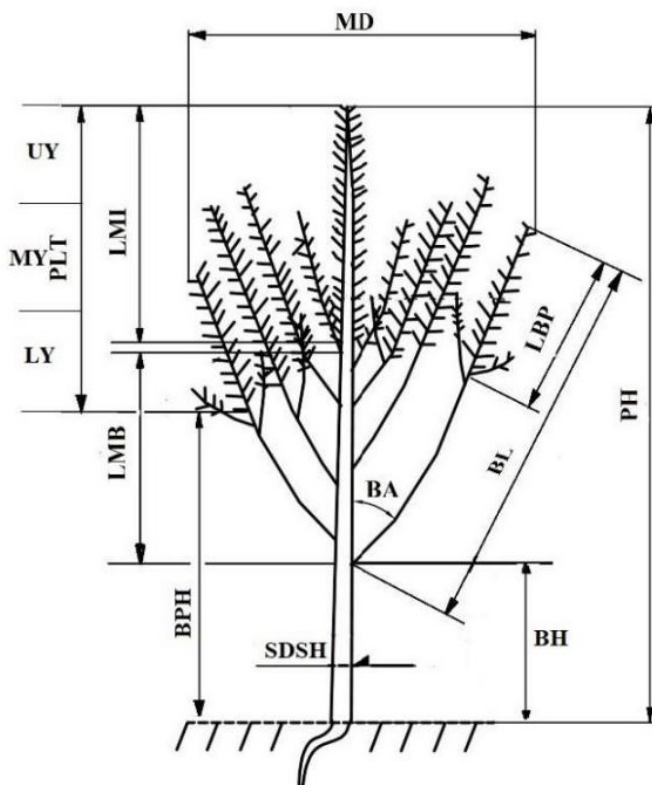
$G_h$  - is the height of the center of gravity of rapeseed plants above the stubble height in mm, and,

H - is the height of rapeseed plants above the stubble height, again in mm.

Based on preliminary experiments and previous research, the relevant parameters required for characterizing the 3D structural features of rapeseed plants have been identified (Figure 2). The plant height (PH), the length of the main stalk with branches (LMB), the length of the main inflorescence (LMI), the stalk diameter at stubble height (SDSH), the bottom pod height (BPH), the maximum diameter of the pod layer (MD), the pod layer thickness (PLT), and branch number (BN) were measured between 9:00 and 11:00 AM using a digimatic caliper (accuracy 0.01 mm) and a tape measure. All measurements were performed by a single trained researcher to ensure consistency, and each parameter was measured three times per plant, with the average value used for subsequent analysis. Damaged or incomplete plants were excluded from the sampling process. The primary branching was counted, and each branch was named—first branch, second branch, etc.—in order from bottom to top.



Figure 1. Shiyezhou experimental field



PH - Plant height; LMB - Length of the main stalk with branches; LMI - Length of the main inflorescence; SDSH - Stalk diameter at stubble height; BPH - Bottom pod height; MD - Maximum diameter of the pod layer; PLT - Pod layer thickness; BN - Branch number; BA - Branch angle; BH - Branch height; BL - Branch length; LBP - Lengths of branches with pods; PNB - Pod number of branches; UL - Upper layer; ML - Middle layer; LL - Lower layer

**Figure 2.** Rapeseed plant characteristics

Branching character is one of the important factors affecting the 3D structure of the rapeseed plant; however, the BN of rapeseed plants is large, as are the differences between each branch of a single plant, so it is not practical to analyze the correlation between the branch characteristics of different plants. Therefore, three rapeseed plants were randomly selected from a total of 25 plants, and the branch angle (BA), branch height (BH), branch length (BL), lengths of branches with pods (LBP), and pod number of branches (PNB) for each branch of a single rapeseed plant were measured using a protractor and a tape measure (Figure 2).

The pod characteristics at different growing positions of a single rapeseed plant differ; therefore, ten representative rapeseed plants with good growth were selected from the 25 plants. The rape pod layer was divided into an upper layer (UL), a middle layer (ML), and a lower layer (LL) according to its thickness (Figure 2), and the pod percentage, pod size, and pod shatter resistance force of each branch and main stalk were measured at different growing positions (UL, ML, LL).

The length, width, and thickness of the pod were measured with a digimatic caliper, with the pod volume being a comprehensive parameter for evaluating pod size. During the experiment, it was noted that the cross section of the pod was similar to an ellipse. Therefore, ignoring the closed curvature of the pod stem end and the pod beak end, the pod shape was described as an elliptical cylinder. The estimation equation of the pod volume  $V$  is obtained according to the length, width, and thickness of the pod (see Eq. 2). Qing (2021b) verified

the accuracy of Eq. 2 using the drainage method, and the error is 2.5%:

$$V = \frac{\pi \times a \times b \times l}{4} \quad (2)$$

where:

- a - is pod width;
- b - is pod thickness, and,
- l - is pod length, all in mm.

Five intact pods were randomly selected from each different growing position and the pod shatter resistance force was measured using the three-point bending suspension fracturing method (Li, 2023). The experiments were carried out on a TA.XTplus texture analyzer (produced in the United Kingdom; the test speed range was 0.01–40 mm s<sup>-1</sup>, the test distance accuracy was 0.001 mm, and the test force accuracy was 0.0002%) in the laboratory at Jiangsu University, as shown in Figure 3. During the test, the pod was suspended on a suspension beam support frame (the span of the support frame was 40 mm, the load acted on the middle point of the span, and the loading speed was 7.8 mm min<sup>-1</sup>). During the test, the load force curve kept rising while the pod remained unshattered, but when the load force reached a certain level, the pod shattered instantaneously, accompanied by a crisp cracking sound. The peak force, i.e., the pod shatter resistance force, was instantly obtained, followed by a rapid decline in the load force curve. The computer dynamically displayed and automatically recorded the peak force.

SPSS 22.0 software was used to describe and statistically analyze the measured data of the 3D structural characteristic parameters of rapeseed plants. The correlation between the 3D structural characteristic parameters was examined using Pearson correlation and linear regression analyses. The

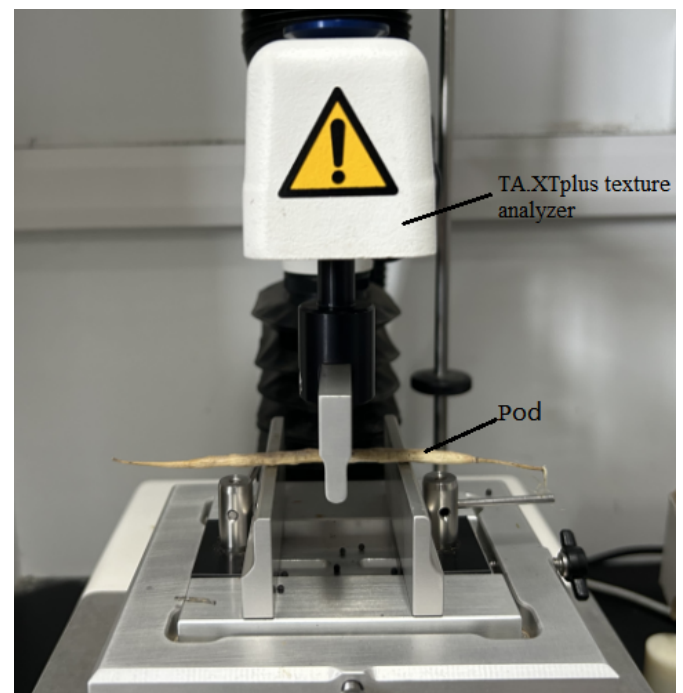


**Figure 3.** Three-point bending suspension fracturing experiment

measured data of the pod characteristic parameters at different growing positions were statistically analyzed by calculating means, and the differences in the pod characteristics at different growing positions were assessed by establishing a three-dimensional bar chart with Origin software (Qing, 2021).

When the reel was working, its motion comprised the forward movement of the combine harvester and the rotary motion of the reel itself (Figure 4). The projection of the reel center shaft axis  $O_0$  on the horizontal ground set the coordinate origin  $O$ , with the  $x$ -axis representing the forward direction of the combine harvester, while the  $y$ -axis through the coordinate origin was perpendicular to the  $x$ -axis. Therefore, the trajectory of a point on the reel can be expressed as in Eq. (3):

$$\begin{cases} x = v_m t + \frac{D}{2} \cos \omega t \\ y = H_1 - \frac{D}{2} \sin \omega t + h \end{cases} \quad (3)$$

where:

- $D$  - is the reel diameter in mm,  $\omega$  is the reel speed in  $\text{rad s}^{-1}$ ,
- $H_1$  - is the reel installation height in mm;
- $h$  - is the stubble height in mm,
- $t$  - is the reel movement time in s, and,
- $V_m$  - is the combine harvester forward speed in  $\text{mm s}^{-1}$ .

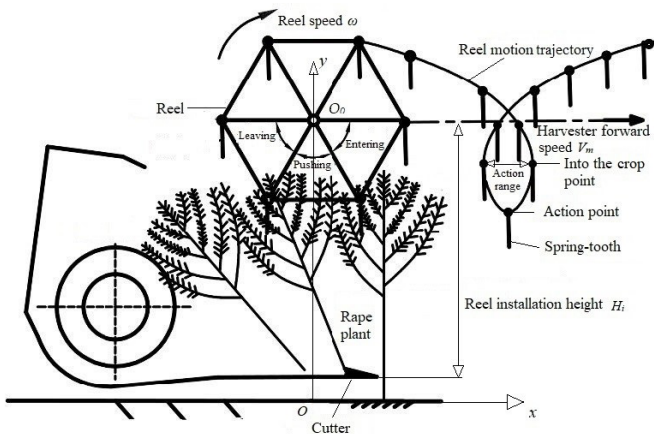


Figure 4. Schematic diagram of reel operation process

## RESULTS AND DISCUSSION

Above the stubble height, the plant height, the height of the center of gravity, and its relative position were measured (Table 1). The relative position of the height of the center of gravity of rapeseed plants was described and analyzed statistically (Table 2). The mean value, the standard deviation, and the variation coefficient of the relative position were 0.61870, 0.024927, and about 4.0%, respectively, indicating that the relative position was less dispersed and relatively stable. Thus, the relative position can be approximated 8/13.

The minimum value, maximum value, average value, standard value, and variable coefficient of 3D structural

Table 1. Relative position of the height of the center of gravity

Number	Plant height (cm)	Height of center of gravity (cm)	Relative position
1	151	93	0.616
2	116	72	0.621
3	112	68	0.607
4	155	97	0.626
5	135	92	0.681
6	121	74	0.612
7	158	92	0.582
8	139	86	0.619
9	128	78	0.609
10	127	78	0.614

characteristic parameters of rapeseed plants, such as PH, LMB, and LMI, were statistically analyzed (Table 3). The variation coefficients (VC) of different 3D structural characteristic parameters ranged from 9.3 to 41.9%, indicating that the 3D structural characteristics of rapeseed plants of the same variety and in the same field were complex and highly variable. Notably, LMB, LMI, and MD exhibited the highest variability ( $VC > 35\%$ ), which can be attributed to the tree-like structure of rapeseed plants. This complex architecture makes these traits particularly susceptible to environmental influences (Qing, 2021), and this pronounced heterogeneity, even within a uniform genetic background, underscores the significant challenge it poses for mechanized harvesting and highlights the critical need for harvester reels that are capable of adapting to such a wide spectrum of plant architectures.

It can be seen in Table 3 that rapeseed plant heights ranged from 142 to 193 cm, with an average value of 168.04 cm, while the standard deviation was 15.574 cm and the plant height variation was 51 cm. Based on the obtained relative position  $C$  of 8/13, the change in the height of the center of gravity was 31.4 cm. Therefore, above stubble height, the change in plant height was 20 cm more than that of the height of the center of gravity, indicating that the variation in plant height and center of gravity height was quite different.

Pearson correlation analysis was performed for different 3D structural characteristic parameters (Table 4), and the false discovery rate (FDR) was the multiple comparison correction method used. PH, LMI, and SDSH were significantly positively correlated with all characteristics. LMB, MD, and BN were not correlated with BPH, but they were positively correlated with other characteristic parameters.

According to the real-time monitoring of the changes in 3D structural characteristic parameters of rapeseed plants, the reel parameters of a combine harvester can be adjusted to improve its performance. The rapeseed plants were tree-like, and the adjacent plants were staggered and shielded each other. Currently, the physical plant properties of crops harvested in the field are generally monitored based on machine vision technology (Niu et al., 2024), which makes it difficult to monitor rapeseed plant characteristics such as the PLT

Table 2. Descriptive statistics analysis of relative position

Minimum Value	Maximum Value	Average value	Standard value	Skewness	Kurtosis	Variable coefficient (%)
0.582	0.681	0.61870	0.024927	0.687	1.334	4.0

**Table 3.** Descriptive statistics analysis of 3D structural characteristic parameters of rapeseed plants

Parameter	Minimum value	Maximum value	Average value	Standard value	Skewness	Kurtosis	Variable coefficient (%)
PH	142	193	168.04	15.574	-0.003	-1.181	9.3
LMB	16	78	38.67	16.186	1.136	1.119	41.9
LMI	42	72	60.71	8.518	-0.763	-1.07	41.0
SDSH	10	30	17.66	5.668	0.739	-0.456	32.1
BPH	88	123	103.08	8.997	0.339	0.058	8.7
MD	30	135	59.96	23.053	1.588	3.858	38.4
PLT	42	80	62.46	10.648	-0.492	-0.174	17.0
BN	4	14	7.67	2.390	1.037	1.635	31.2

PH - Plant height; LMB - Length of the main stalk with branches; LMI - Length of the main inflorescence; SDSH - Stalk diameter at stubble height; BPH - Bottom pod height; MD - Maximum diameter of the pod layer; PLT - Pod layer thickness; BN - Branch number

**Table 4.** Pearson correlation analysis of 3D structural characteristic parameters of rapeseed plants

Parameter	PH	LMB	LMI	SDSH	BPH	MD	PLT	NB
PH	1	0.767**	0.859**	0.839**	0.674**	0.674**	0.852**	0.712**
LMB	0.767**	1	0.668**	0.884**	0.324	0.820**	0.766**	0.932**
LMI	0.859**	0.668**	1	0.657**	0.492*	0.574**	0.901**	0.659**
SDSH	0.839**	0.884**	0.657**	1	0.468*	0.855**	0.779**	0.853**
BPH	0.674**	0.324	0.492*	0.468*	1	0.348	0.349	0.260
MD	0.674**	0.820**	0.574**	0.855**	0.348	1	0.698**	0.776
PLT	0.852**	0.766**	0.901**	0.779**	0.349	0.698**	1	0.722**
BN	0.712**	0.932**	0.659**	0.853**	0.260	0.776**	0.722**	1

Note: \* Significant at  $p \leq 0.05$  by t-test, \*\* Extremely significant at  $p \leq 0.01$  by t-test; PH - Plant height; LMB - Length of the main stalk with branches; LMI - Length of the main inflorescence; SDSH - Stalk diameter at stubble height; BPH - Bottom pod height; MD - Maximum diameter of the pod layer; PLT - Pod layer thickness; BN - Branch number

directly. Therefore, based on the Pearson correlation between different characteristic parameters, the linear regressions models between different characteristic parameters were analyzed, which provided the theoretical basis for the real-time monitoring of the 3D structural characteristics of rapeseed plants in the future.

The closer the correlation coefficient is to 1, the closer the linear relationship between the two parameters is; therefore, when the correlation coefficient between different parameters was  $\geq 0.8$ , the relationship between the two parameters was considered to be linear (Qing, 2021). As can be seen in Table 4, the following parameters were closer to linear correlation: PH and LMI (0.859), PH and SDSH (0.839), PH and PLT (0.852), LMB and BN (0.932), LMB and SDSH (0.884), LMB and MD (0.820), LMI and PLT (0.901), SDSH and MD (0.855), and SDSH and BN (0.853). Table 5 exhibits the linear regression models between different parameters.

Three rapeseed plants were randomly selected to measure each BA, BL, BH, LBP, and PNB, and the measurement data were used for carrying out descriptive statistical analysis, as shown in Table 6. The variation coefficient of BA was less than 10%, indicating that the degree of variation was small. The characteristic parameters of each branch, such as BH, BL,

LBP, and PNB, showed obvious changes (Figure 5). The BH increased and the BL decreased linearly with the rise in branch order. The LBP increased first and then decreased, while the LBP of top- and bottom-part branches was shorter, and that of middle-part branches was longer. The PNB showed a tendency towards fewer pods in top- and bottom-part branches and more pods in middle-part branches. This was consistent with the variation in the LBP.

As can be seen in Figure 6, from the overall perspective of the pod growing position, the pod number percentages of UL, ML, and LL were 39.68, 49.02, and 11.3%, respectively. The pod number percentage of ML was  $>$  that of UL, which was  $>$  that of LL. According to the pod growing position of each branch, the order of the pod number percentage distribution (in descending order) was as follows: main branch ML  $>$  third branch UL  $>$  main branch UL  $>$  fourth branch UL = seventh branch ML  $>$  sixth branch ML  $>$  sixth branch UL  $>$  first branch ML  $>$  third branch ML  $>$  second branch ML  $>$  seventh branch UL  $>$  second branch UL = main branch LL  $>$  fourth branch UL  $>$  first branch UL  $>$  sixth branch UL  $>$  other branches LL.

Figure 7 shows that, from the overall perspective of the pod growing position, the average volumes of UL, ML, and LL were 1637, 1882, and 1666 mm<sup>3</sup>, respectively. The pod volume

**Table 5.** Linear regression models between different parameters

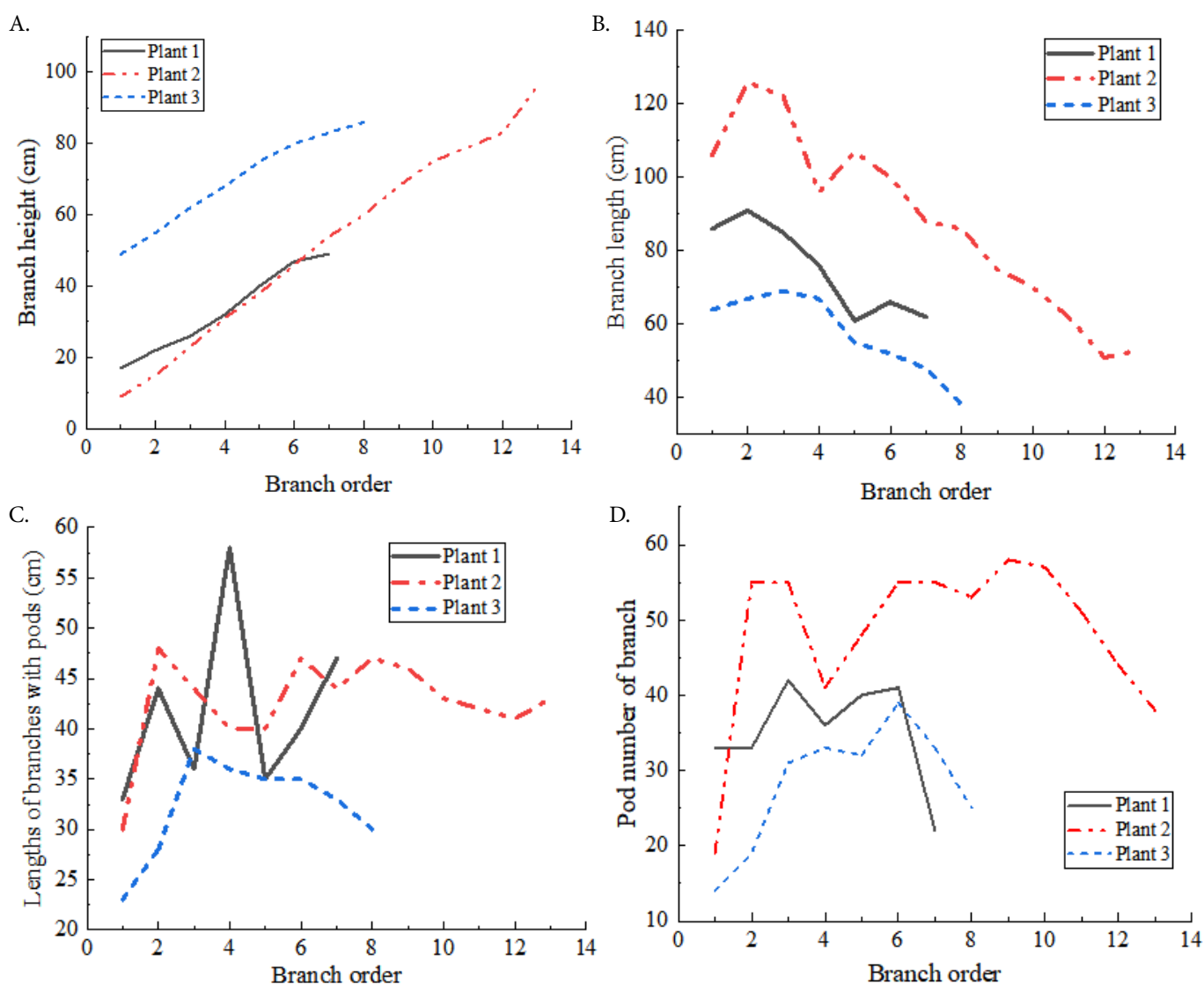
Parameter – Parameter	F-test	Model	R <sup>2</sup> Value
PH – LMI	62.137**	LMI=0.47*PH-18.277	0.739
PH – SDSH	50.070**	SDSH=0.313*PH-34.669	0.705
PH – PLT	58.220**	PLT=0.582*PH-35.42	0.726
LMB – BN	146.151**	BN=0.138*LMSB+2.345	0.869
LMB – SDSH	75.181**	SDSH=0.304*LMSB+5.999	0.782
LMB – MD	45.257**	MD=1.168*LMSB+14.782	0.673
LMI – PLT	94.613**	PLT=1.126*LMI-5.898	0.811
SDSH – MD	57.035**	MD=3.466*SDSH-2.32	0.731
SDSH – BN	56.004**	BN=0.36*SDSH+1.213	0.727

Note: \* Significant at  $p \leq 0.05$  by F-test, \*\* Extremely significant at  $p \leq 0.01$  by F-test; PH - Plant height; LMB - Length of the main stalk with branches; LMI - Length of the main inflorescence; SDSH - Stalk diameter at stubble height; BPH - Bottom pod height; MD - Maximum diameter of the pod layer; PLT - Pod layer thickness; BN - Branch number

**Table 6.** Descriptive statistics analysis of branching characteristic parameters

No.	BN	Parameter	Minimum value	Maximum value	Average value	Standard value	Skewness	Kurtosis	Variable coefficient (%)
Plant 1	7	BA	33	39	35.86	1.952	0.277	0.042	0.05
		BH	17	49	33.29	12.433	0.075	-1.732	0.37
		BL	61	91	75.29	12.406	-0.004	-2.183	0.16
		LBP	33	58	41.86	8.707	1.106	0.948	0.21
		PNB	22	63	38.75	11.708	1.093	2.890	0.30
Plant 2	13	BA	35	50	42.54	4.196	-0.016	-0.161	0.10
		BH	9	96	52.08	27.705	-0.081	-1.168	0.53
		BL	51	126	87.85	24.596	-0.044	-1.048	0.28
		LBP	30	48	42.69	4.644	-1.710	4.278	0.11
Plant 3	8	PNB	19	93	52.29	15.404	0.707	4.850	0.29
		BA	38	50	44.75	4.200	-0.322	-0.379	0.09
		BH	49	86	69.75	13.541	-0.366	-1.344	0.19
		BL	38	69	57.50	11.097	-0.689	-0.621	0.19
		LBP	23	38	32.25	4.950	-0.934	0.286	0.15
		PNB	14	39	28.25	8.294	-0.731	-0.313	0.29

BA - Branch angle; BH - Branch height; BL - Branch length; LBP - Lengths of branches with pods; PNB - Pod number of branches

**Figure 5.** The effect of branching order on branching characteristic variables

of ML was the largest and that of UL was similar to that of LL. According to the pod growing position of each branch, a pod volume > 2000 mm<sup>3</sup> was the first order, including the first branch UL and ML, the second branch LL, the third branch ML, and the fourth branch ML. The pod volume in the range

of 1600–2000 mm<sup>3</sup> was the second order, including the second branch UL and ML, the third branch UL and LL, the fourth branch UL and LL, the sixth branch UL, and the main branch ML and LL. The remaining pod volume of less than 1600 mm<sup>3</sup> was the third order.

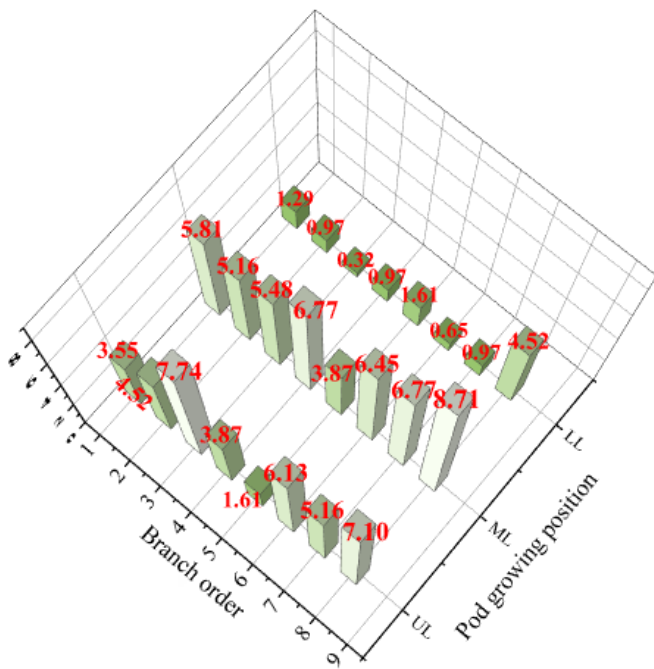


**Figure 6.** Pod number percentage in different growing positions

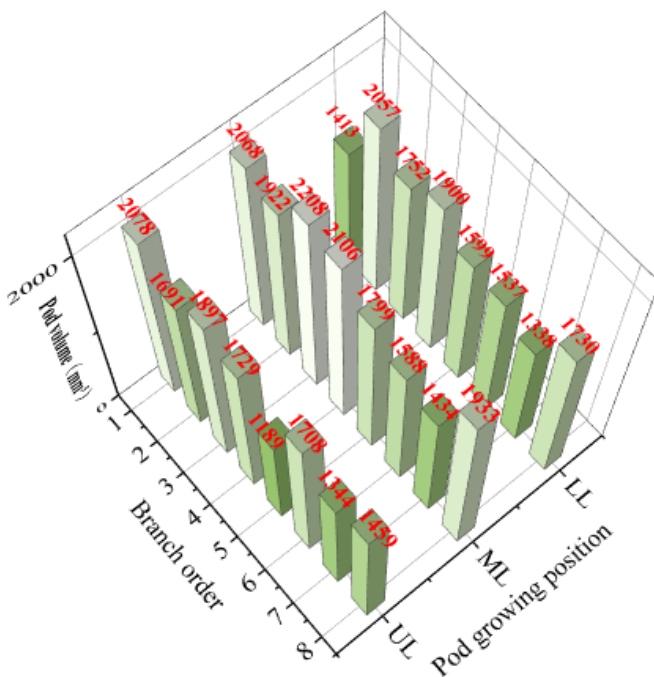


**Figure 7.** Pod volume in different growing positions

As depicted in Figure 8, from the overall perspective of the pod growing position, the average pod shatter resistance forces of UL, ML, and LL were 1.13 N, 1.96 N, and 1.54 N, respectively. The pod shatter resistance force of ML was > that of LL, which was > that of UL. In the optimum period for harvesting rape with a combine harvester, the maturity of rape pod was higher, and the pod shatter resistance force diminished with the decrease in pod moisture content and rose with the increase in rape volume (Li et al., 2012). This may have been because the UL pod had less shelter, while both sunshine and ventilation were better than for the ML and LL pod, and the LL pod had better ventilation than the ML pod, resulting in the ML pod moisture content being > the LL pod moisture

content, which was > the UL pod moisture content. Based on the pod growing position of each branch, the shatter resistance forces of the UL pod in the top-part branches and the LL pod in the bottom-part branches were significantly lower than those for other growing positions. As mentioned above, this may be because the pod volume of these parts of the growing position was small. Although the LL pod of the second branch had a larger volume, this may be due to the better ventilation of the LL pod of the bottom-part branches, which led to the lower moisture content of the pod. Qing (2021) found that the pod moisture content had more influence on the pod shatter resistance force than the pod volume for a single rapeseed plant.

During the operation of a rape combine harvester, the reel motion trajectory should meet the following two requirements: 1) that its crop point is at the highest point of the crop itself; and 2) that its action point is slightly above the center of gravity height of the cut crop (Qing, 2021). If the crop point and the action point of the reel are too high, it will lead to the weakening of the reel effect; if they are too low, it may lead to multiple collisions between the crop and the reel, or even the whole plant being lifted by the reel and thrown out of the cutting table. The field measurement data indicated that the height of rapeseed plant 1 was 1400 mm, the harvester forward speed was 1000 mm s<sup>-1</sup> (1 m s<sup>-1</sup>), and the stubble height was 350 mm. Because of the height of rapeseed plant 1, it was necessary to adjust the installation height, the speed, and the diameter of the reel, so that the reel motion trajectory met the above two requirements at the same time (Figure 9). When the height of rapeseed plant 2 changed to 1700 mm, it was found that the reel motion trajectory could not meet one of the above two requirements if the parameters of the reel were not adjusted. The traditional reel diameter was determined according to the average of the height of rapeseed plants and the height of the center of gravity above the stubble height, and this was corrected and not adjustable (Jin et al., 2023). The installation

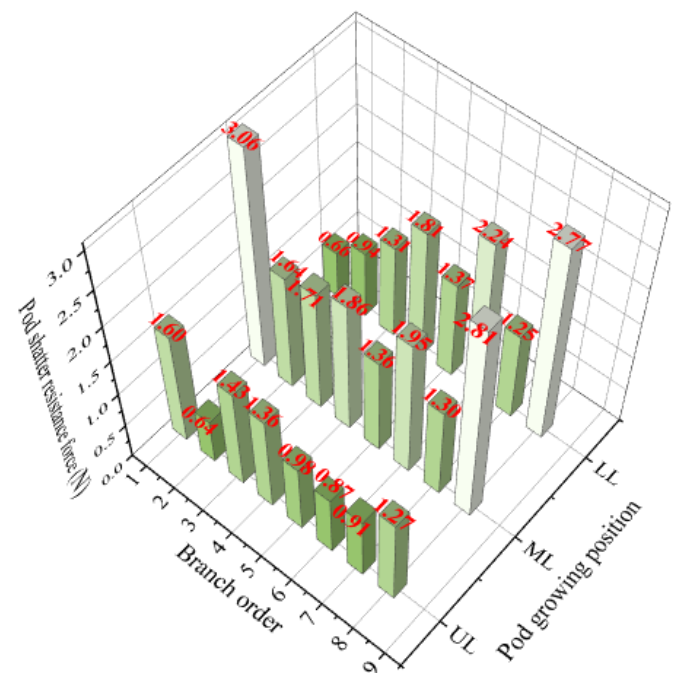
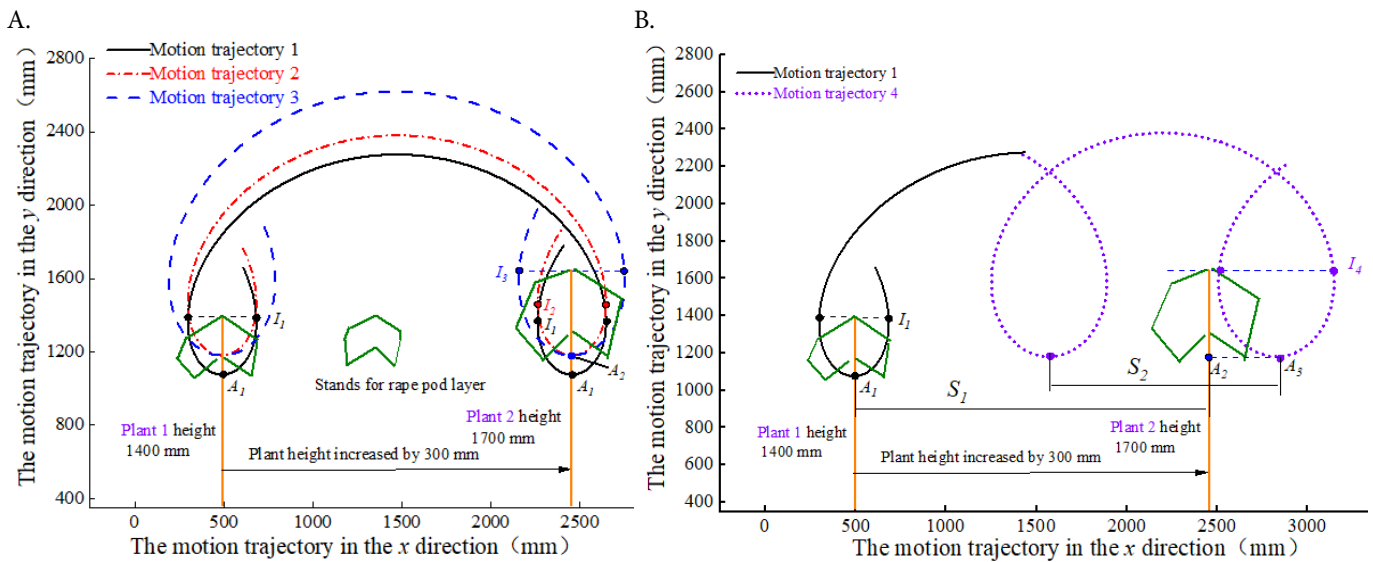


**Figure 8.** Pod shatter resistance force in different growing positions



$I_1$ ,  $I_2$ , and  $I_3$  - Are the crop points of motion trajectories 1, 2, and 3, respectively;  $A_1$  - Is the action point of motion trajectory 1;  $A_2$  - Is the action point of motion trajectories 2 and 3;  $I_4$  - Is the crop point of motion trajectory 4;  $S_1$  - Is the pitch of the buckle ring of motion trajectories 1, 2, and 3, mm;  $S_2$  - Is the pitch of the buckle ring of motion trajectory 4, in mm

**Figure 9.** Analysis of reel motion trajectory

height of the traditional reel was only adjusted to make reel motion trajectory 2 adapt to the change of the rapeseed plant height. As shown in Figure 9, if the action point of reel motion trajectory 2 meets the requirement while the crop point does not, only one of the two requirements can be satisfied. However, by adjusting the installation height and diameter of the reel to change to reel motion trajectory 3, both requirements can be met.

As Figure 9 shows, the two requirements can also be met by adjusting the installation height and the speed of the reel; however, raising the reel speed will increase the number of collisions between the reel and the rapeseed plant per unit time. Moreover, by adjusting the reel speed, the pitch between the buckle rings will be altered, which will easily lead to a shift in the reel action point and the position slightly above the center of gravity in the x direction, thereby reducing the performance of the reel. Therefore, in order to better adapt the reel motion trajectory to the change in the height of the rapeseed plant, the reel diameter must be taken into account in future research.

With regard to the above findings, the aim of the analysis was to reduce the number of times the reel hit the pod growing position with little shatter resistance. In terms of the pod number, the reel must be reduced to strike the UL and ML pods of the main stalk and top-part branches. And as for the pod shatter resistance force, the reel must be minimized to strike the UL pods of the main stalk and top-part branches, and the LL pods of the bottom-part branches. However, the percentage of the LL pods in the bottom-part branches was relatively small, at only about 1%; therefore, the impact on the UL pods of the main stalk and top-part branches should be reduced in future research on reel motion trajectories and sprung-teeth angles.

Based on the above results and discussion, in terms of motion trajectories 1 and 2, it can be seen that when the plant height increased, the blow of the reel on the UL pods of the main stalk and top-part branches was significantly greater without adjusting the reel parameters or only altering the reel installation height. This once again confirmed the importance of the adaptability of the reel in a rape combine

harvester. Future work will focus on the design and validation in the field of reels with adjustable diameters and installation heights.

## CONCLUSIONS

1. For Ningza 158, the center of gravity averages 8/13 of the plant height ( $n = 10$ , need replication).
2. Some 3D parameters of rapeseed plants correlate strongly (9 out of 28 pairs), suggesting the potential for indirect measurement.
3. Theoretical trajectory analysis indicates that coordinated height and diameter adjustment of the reel might improve harvester performance, which warrants experimental testing.

**Author contributions:** Yanbin Liu contributed to the design of the research, the collection, analysis, and interpretation of data, administration and the acquisition of financing, and the preparation of the manuscript; Yaoming Li contributed to the design of the research, and the collection, analysis, and interpretation of data; Tiaotiao Chen contributed to the supervision of the work and administration; Zhenwei Liang contributed to the design of the research, and the collection, analysis, and interpretation of data; Li Zeng contributed to the design of the research, and the collection, analysis, and interpretation of data.

**Data availability statement:** Data underlying the text of this article are available on request from the corresponding author.

**Conflict of interest:** The authors declare no conflicts of interest.

**Financing statement:** The study was funded by the Youth Project of the Natural Science Foundation of Jiangsu Province (No. BK20240879), the China Postdoctoral Science Foundation (2024M761843), the Shandong Province Postdoctoral Innovation Project (No. SDCX-ZG-202400199), the Major Scientific and Technological Special Project of Anhui Province (No. 202203a06020025), and the Jiangsu Agricultural

Science and Technology Independent Innovation Fund (No. CX(C21)2042).

## LITERATURE CITED

- Delgado, M.; Felix, M.; Bengoechea, C. Development of bioplastic materials: from rapeseed oil industry by products to added-value biodegradable biocomposite materials. *Industrial Crops & Products*, v.166, e113459, 2021. <https://doi.org/10.1016/j.indcrop.2018.09.013>
- Du, C.; Han, D.; Song, Z.; Chen, Y.; Chen, X.; Wang, X. Calibration of contact parameters for complex shaped fruits based on discrete element method: The case of pod pepper (*Capsicum annuum*). *Biosystems Engineering*, v.226, p.43-54, 2023. <https://doi.org/10.1016/j.biosystemseng.2022.12.005>
- Guo, H.; Guo, L.; Li, H.; Dong, Y.; Zhou, W.; Han, J. Calibration and experiment of the discrete element simulation parameters for rapeseed stems during the suitable harvest period. *Transactions of the Chinese Society of Agricultural Engineering*, v.40 p.20-29, 2024. <https://doi.org/10.11975/j.issn.1002-6819.202408199>
- Hu, Y.; Wang, S.; Li, B.; Guo, X.; Chen, S. The influence of the distribution law and uniformity of a threshed mixture with the working parameters of a soybean threshing device. *Agronomy*, v.14, e1581, 2024. <https://doi.org/10.3390/agronomy14071581>
- Ji, K.; Li, Y.; Liang, Z.; Liu, Y.; Cheng, J.; Wang, H.; Zhu, R.; Xia, S.; Zheng, G. Device and method suitable for matching and adjusting reel speed and forward speed of multi-crop harvesting. *Agriculture*, v.12, e213, 2022. <https://doi.org/10.3390/agriculture12020213>
- Jin, C.; Qi, Y.; Liu, G.; Yang, T.; Ni, Y. Mechanical analysis and parameter optimization of soybean combine harvester reel. *Transactions of the Chinese Society of Agricultural Machinery*, v.54, p.104-113, 2023. <https://doi.org/10.6041/j.issn.1000-1298.2023.06.011>
- Jing, T.; Tang, Z.; Hao, S.; Shen, C.; Wang, T.; Wang, M. Structure design and rice threshing performance of the variable-speed inertial pulley for simulating artificial threshing. *International Journal of Agricultural and Biological Engineering*, v.17, p.33-40, 2024. <https://doi.org/10.25165/j.ijabe.20241701.8325>
- Li, G. Key technology research and mechanism optimisation for plucking and damage reduction during oilseed rape harvest. *Chinese Academy of Agricultural Sciences*, 2023. <https://doi.org/10.27630/d.cnki.gznky.2023.000692>
- Li, Y.; Wan, X.; Liao, Q.; Liu, Y.; Zhang, Q.; Liao, Y. Design and experiment of wide folding rape windrower based on crawler type power chassis. *Journal of Jilin University*, v.54, p.3740-3754, 2024. <https://doi.org/10.3969/j.issn.1002-6819.2012.08.017>
- Li, Y.; Zhu, J.; Xu, L.; Zhao, Z. Experiment on strength of rapeseed pod dehiscence based on impending fracturing method. *Transactions of the Chinese Society of Agricultural Engineering*, v.28, p.111-115, 2012. <https://doi.org/10.13229/j.cnki.jdxbgxb.20230122>
- Luo, H.; Jin, Y.; Tong, X.; Wu, M.; Song, X.; Jiang, X. Design and testing of air-blown low-loss seed recovery nozzles for oilseed rape combine harvester cutting decks. *Transactions of the Chinese Society for Agricultural Machinery*, v.56, p.267-278, 2025.
- Ma, L.; Wei, J.; Huang, X.; Zong, W.; Zhan, G. Analysis of harvesting losses of rapeseed caused by vibration of combine harvester header during field operation. *Transactions of the Chinese Society of Agricultural Machinery*, v.51, p.134-138, 2020. <https://doi.org/10.6041/j.issn.1000-1298.2020.S2.016>
- Niu, Y.; Han, W.; Zhang, H.; Zhang, L.; Chen, H. Estimating maize plant height using a crop surface model constructed from UAV RGB images. *Biosystems Engineering*, v.241, p.56-57, 2024. <https://doi.org/10.1016/j.biosystemseng.2024.04.003>
- Qing, Y. Study on pod shatter resistance, plant type structure and reel mechanism for low-loss mechanized harvesting. *Jiangsu University*, 2021. <https://doi.org/10.27170/d.cnki.gjsuu.2021.000137>
- Qing, Y.; Li, Y.; Xu, L.; Ma, Z. Screen oilseed rape (*brassica napus*) suitable for low-loss mechanized harvesting. *Agriculture*, v.11, e504, 2021a. <https://doi.org/10.3390/agriculture11060504>
- Qing, Y.; Li, Y.; Xu, L.; Ma, Z.; Tan, X.; Wang, Z. Oilseed rape (*Brassica napus* L.) pod shatter resistance and its relationship with whole plant and pod characteristics. *Industrial Crops & Products*, v.166, e113459, 2021b. <https://doi.org/10.3390/agriculture14050777>
- Que, K.; Tang, Z.; Wang, T.; Su, Z.; Ding, Z. Effects of unbalanced incentives on threshing drum stability during rice threshing. *Agriculture*, v.14, e777, 2024. <https://doi.org/10.3390/agriculture14050777>
- Shu, C.; Yang, J.; Wan, X.; Yuan, J.; Liao, Y.; Liao, Q. Calibration and experiment of the discrete element simulation parameters of rape threshing mixture in combine harvester. *Transactions of the Chinese Society of Agricultural Engineering*, v.38, p.34-43, 2022. <https://doi.org/10.11975/j.issn.1002-6819.2022.09.004>
- Sun, X.; Zong, W.; Wei, X. DEM-MBD coupling-based analysis and experiment on loss reduction mechanisms of rapeseed pickup header in hilly and mountainous areas. *Computers and Electronics in Agriculture*, v.238, e110817, 2025. <https://doi.org/10.1016/j.compag.2025.110817>
- Tang, Z.; Zhang, B.; Wang, B.; Wang, M.; Chen, H.; Li, Y. Breaking paths of rice stalks during threshing. *Biosystems Engineering*, v.204, p.346-357, 2021a. <https://doi.org/10.1016/j.biosystemseng.2021.02.008>
- Tang, Z.; Zhang, B.; Wang, M.; Zhang, H. Damping behaviour of a prestressed composite beam designed for the thresher of a combine harvester. *Biosystems Engineering*, v.204, p.130-146, 2021b. <https://doi.org/10.1016/j.biosystemseng.2021.01.020>
- Wang, W.; He, Z.; Zhang, R.; Li, M.; Xu, Z.; Xiang, X. The influence of *Lactobacillus plantarum* fermentation in selenium-enriched *Brassica napus* L.: changes in the nutritional constituents, bioactivities and bioaccessibility. *Oil Crop Science*, v.9, p.81-90, 2024. <https://doi.org/10.1016/j.ocsci.2024.03.004>
- Yuan, J.; Wan, X.; Liao, Q.; Gao, D.; Xiao, W.; Yang, J. Mechanical compression characteristics of rapeseed based on continuous damage theory. *Biosystems Engineering*, v.224, p.301-312, 2022. <https://doi.org/10.1016/j.biosystemseng.2022.10.008>
- Zhao, Y.; Tang, Z.; Chen, S. Loading model and mechanical properties of mature broccoli (*Brassica oleracea* L. Var. Italica Plenck) stems at harvest. *Agriculture*, v.12, e1519, 2022. <https://doi.org/10.3390/agriculture12101519>
- Zhou, W.; Wang, Z.; Guan, R.; Wang, J.; Sun, X. A multi-scale model for postharvest mechanical damage in carrots: Bridging viscoelastic-plastic theory and bonded particle optimization with DEM. *Postharvest Biology and Technology*, v.231, e113879, 2026. <https://doi.org/10.1016/j.postharvbio.2025.113879>